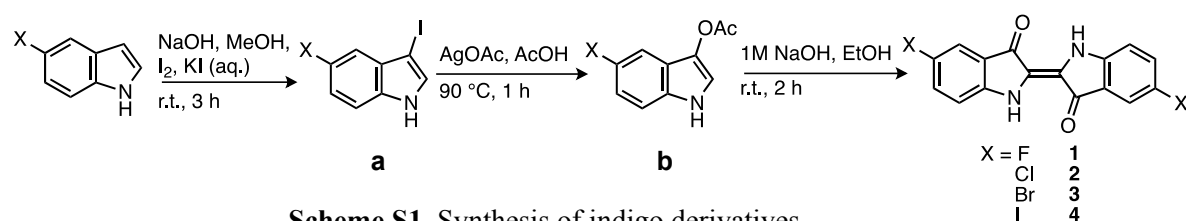**Supporting Information**

Iodine Effect in Ambipolar Organic Field-Effect Transistors Based on Indigo Derivatives

Oratai Pitayatanakul,[*a] *Kodai Iijima,*[a] *Minoru Ashizawa,*[a] *Tadashi Kawamoto,*[a] *Hidetoshi Matsumoto,*[a] *and Takehiko Mori*[*ab]

Synthesis

Scheme S1. Synthesis of indigo derivatives.

Compounds **1-4** were prepared following Scheme S1 similarly to 5,5'-diphenylindigo.[9] The iodination, followed by acetoxylation with silver acetate in acetic acid to afford 5-halogenoacetoxyindole (X = F, Cl, Br, and I). The alkaline hydrolysis accompanied by air oxidation gave the corresponding **1-4** of 5,5'-dihalogenoindigo.[19,20] The data of Nuclear Magnetic Resonance spectrum (NMR) and Mass spectrum (MS) were obtained with a JEOL JNM-AL300 spectrometer and a GC–MS-QP-5000 Shimadzu Mass Spectrometer, respectively. Wakogel® C-200 was used as a filler for column chromatography. For the sublimation process of **1**, **2**, and **4**, the glass tubes were heated for about 24 h under a vacuum of 10^{-4} Pa in the temperature range of 270°C~350°.

5-Halogeno-3-iodoindole (a). To a solution of 5-halogenoindole (1.02 mmol) and sodium hydroxide (41 mg, 1.02 mmol) in methanol (10 ml) were added iodine (259 mg, 1.02 mmol) and an aqueous solution (2 ml) of potassium iodide (169 mg, 1.02 mmol). After the mixture was stirred at room temperature for 3 h, water was added. The resulting precipitate was collected by filtration, washed with water, and dried to give 5-halogeno-3-iodoindole, which was used for the following reaction without purification because of its instability.

X = **F**; 76% with no purification; white solid; EIMS m/z: 261 [M$^+$]; ^{1}H NMR (300 MHz, CDCl$_3$, δ): 8.37 (broad, 1H, NH), 7.33 (d, 1H, Ar H), 7.28 (t, 1H, Ar H), 7.15 (dd, 1H, Ar H), 7.03 (m, 1H, Ar H).

X = **Cl**; 85% with no purification; pink (purple) solid; EIMS *m/z*: 279 [M + 2], 277 [M$^+$]; ^{1}H NMR (300 MHz, CDCl$_3$, δ): 8.38 (broad, 1H, NH), 7.45 (t, 1H, Ar H), 7.31 (d, 1H, Ar H), 7.28 (dd, 1H, Ar H), 7.18 (m, 1H, Ar H).

X = **I**; 88% with no purification; orange (brown) solid; EIMS *m/z*: 369 [M$^+$]; ^{1}H NMR (300 MHz, CDCl$_3$, δ): 8.4 (broad, 1H, NH), 7.8 (d, 1H, Ar H), 7.5 (dd, 1H, Ar H), 7.25 (m, 1H, Ar H), 7.14 (d, 1H, Ar H).

3-Acetoxy-5-halogenoindole (b). Silver acetate (327.6 mg, 1.96 mmol) was added to a solution of 5-halogeno-3-iodoindole (0.98 mmol) in acetic acid (8 ml). After stirring at 90°C for 1 h, the mixture was cooled to room temperature and filtrated. The filtrate was evaporated to dryness under reduced pressure. The residue was chromatographed on silica gel with dichloromethane (CH$_2$Cl$_2$) and recrystallized with hexane : ethyl acetate (20 : 1) to give 3-acetoxy-5-halogenoindole.

X = **F**; 33%; light blue solid; EIMS *m/z*: 193 [M$^+$], 151; ^{1}H NMR (300 MHz, CDCl$_3$, δ): 7.83 (broad, 1H, NH), 7.4 (d, 1H, Ar H), 7.18 (m, 2H, Ar H), 6.9 (m, 1H, Ar H), 2.36 (s, 3H, CH$_3$).

X = **Cl**; 30%; colorless solid; EIMS *m/z*: 277, 209 [M$^+$], 167; ^{1}H NMR (300 MHz, CDCl$_3$, δ): 7.9 (broad, 1H, NH), 7.52 (d, 1H, Ar H), 7.36 (d, 1H, Ar H), 7.25 (d, 1H, Ar H), 7.14 (dd, 1H, Ar H), 2.36 (s, 3H, CH$_3$).

X = **I**; 34%; light brown solid; EIMS *m/z*: 301 [M$^+$], 259; ^{1}H NMR (300 MHz, CDCl$_3$, δ): 7.9 (broad, 1H, NH), 7.47 (d, 1H, Ar H), 7.35 (d, 1H, Ar H), 7.28 (m, 1H, Ar H), 7.14 (d, 1H, Ar H), 2.36 (s, 3H, CH$_3$).

5,5'-Dihalogenoindigo (1, 2, and 4). To a solution of 3-acetoxy-5-halogenoindole (2.2 mmol) in ethanol (50 ml) was added aqueous 1 M sodium hydroxide (40 ml). After the mixture was stirred at room temperature for 2 h, water was added. The resulting precipitate was collected by filtration, washed with water, and dried to give 5,5'-dihalogenoindigo. Compounds **1**, **2** and **4** were purified by sublimation under 10^{-4} Pa about 24 h at 270°C, 330°C, and 350°C, respectively.

X = **F (1)**; 44% (crude); dark blue solid; EIMS *m/z*: 298 [M$^+$], 270, 241. Anal. calcd for C$_{16}$H$_8$F$_2$N$_2$O$_2$: C 64.43, H 2.70, F 12.74, N 9.39; found: C 64.67, H 2.47, F 12.94, N 9.47; IR (KBr): v = 3271 (NH), 1627 (C=O), 1595 (Ar), 1481, 1182, 1136, 1105, 1055, 684 cm^{-1}.

X = **Cl (2)**; 59% (crude); dark blue solid; EIMS *m/z*: 330 [M$^+$]; IR (KBr): v = 3281 (NH), 1629 (C=O), 1608 (Ar), 1464, 1188, 1142, 1120, 1041, 642 cm^{-1}.

***X* = I (4)**; 75% (crude); dark blue solid. Anal. calcd for $C_{16}H_8I_2N_2O_2$: C 37.38, H 1.57, I 49.37, N 5.45; found: C 37.75, H 1.71, I 48.8, N 5.44; IR (KBr): ν = 3289 (NH), 1628 (C=O), 1605 (Ar), 1456, 1188, 1138, 1119, 1074, 605 cm^{-1}.

Cyclic Voltammetry (CV) and Ultraviolet-Visible Spectroscopy (UV-Vis)

CV and UV-Vis were measured to determine the HOMO/LUMO levels and energy gaps of the indigo derivatives as shown in Figures S1 and S2. All data are summarized in Table S1. CV scan curves of a 20 nm thin film of **1-4** on an ITO glass were collected on Bi-Potentionstat ALS/DY2323 using Ag in 0.1 M $AgNO_3$ solution for a reference electrode, platinum (Pt) for a working electrode and carbon for a counter electrode in tetrabutylammonium hexafluorophosphate (Bu_4NPF_6) in a benzonitrile (C_6H_5CN) electrolyte solution at a scan rate of 100 mV s^{-1}. HOMO and LUMO energy levels were estimated by assuming the reference energy level of ferrocene/ferrocenium (Fc/Fc$^+$: $E^{1/2}$ = +0.178 V *vs*. Ag/AgNO$_3$ measured under identical conditions) to be 4.8 eV from the vacuum level.[22] UV-Vis spectra were collected on a Jasco Corporation V-630 UV/VIS Spectrophotometer for a 20 nm of thin films evaporated on a glass substrate.

Table S1. Redox potentials and energy levels of thin films of **1-4**.

Compounds	E_{ox} [V]	E_{red} [V]	HOMO [eV]	LUMO [eV]	HOMO-LUMO gap [eV]	Optical gap [eV]
1 (F)	0.68	−1.39	5.48	3.41	2.07	1.66
2 (Cl)	0.44	−1.48	5.24	3.32	1.92	1.72
3 (Br)	0.71	−1.31	5.51	3.49	2.02	1.71
4 (I)	0.64	−1.22	5.44	3.58	1.86	1.68

Onset redox potentials *vs*. Fc/Fc$^+$ are assumed to be 4.8 eV from the vacuum level.[22]
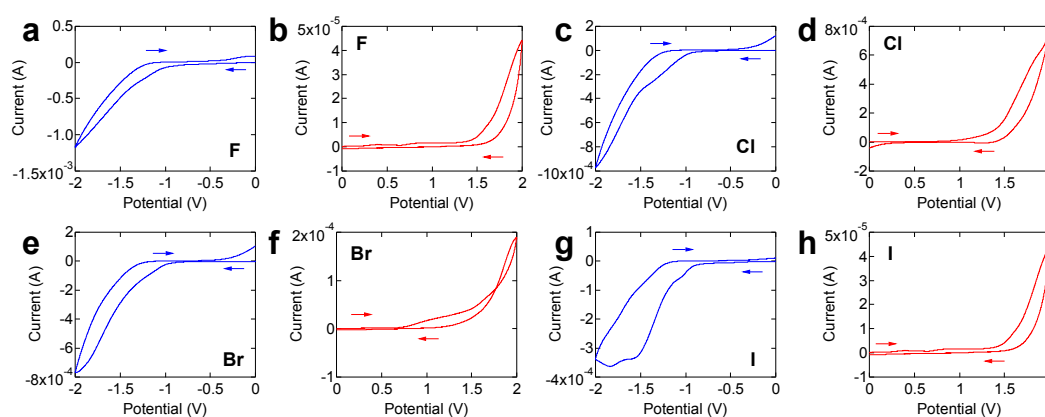Fc/Fc$^+$: $E^{1/2}$ = +0.178 V

Fig. S1. CV scan curves of a 20 nm thin films of (a,b) **1**, (c,d) **2**, (e,f) **3** and (g,h) **4** in a benzonitrile (C_6H_5CN) solution using Pt as a working electrode, carbon as a counter electrode in tetrabutylammonium hexafluorophosphate (Bu_4NPF_6) electrolyte solution *vs*. Ag/AgNO$_3$.
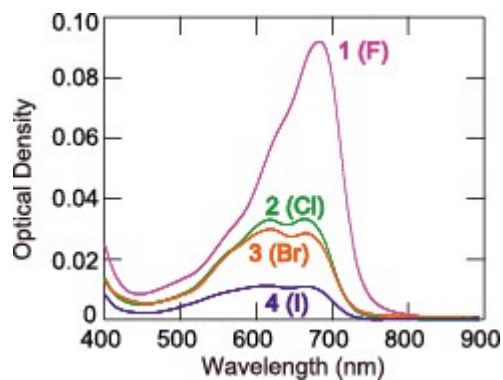
Fig. S2. Optical absorption spectra of **1-4**. UV-vis was measured using a 20 nm thin film evaporated on a glass substrate.

Molecular Orbitals

Molecular orbital calculations were carried out basically similarly to Ref. 5. Molecular orbitals of **1-4** were calculated by Gaussian 09 package at B3LYP/CEP-31G level.[S1] The HOMO and LUMO after the geometrical optimization were shown in Fig. 1. The transfer integrals, t_i, listed in Table 2 were estimated from the intermolecular overlap integrals, S_i as $t_i = E \times S_i$ by assuming the energy level E to be -10 eV.[S2]

Crystal Structures

Crystal structures of **1** and **3** have been recently reported.[9,10] In the present work, we show our data of **2** and **4** in comparison with the reported data of **1** and **3** in Table S2. Crystals grown by the nitrogen flow method were used for the X-ray single-crystal structure analyses (Table S2). The diffraction data of **2** and **4** were collected by a RIGAKU R-AXIS RAPID II imaging plate with Cu-$K\alpha$ radiation from a rotation anode source with a confocal multilayer X-ray mirror (RIGAKU VM-Spider, λ = 1.54187 Å). The structures of **2** and **4** were solved by the direct method (SIR2008) and refined by the full matrix least-squares procedure (SHELXL).[S3,S4] Anisotropic thermal parameters were adopted for all non-hydrogen atoms.

Table S2. Crystallographic data of **1-4**.

Compound	**1** (F)[10]	**2** (Cl)	**3** (Br)[9]	**4** (I)
Chemical formula	$C_{16}H_8N_2O_2F_2$	$C_{16}H_8N_2O_2Cl_2$	$C_{16}H_8N_2O_2Br_2$	$C_{16}H_8N_2O_2I_2$
Formula weight	298.24	331.15	420.05	514.06
Shape	Dark blue non-transparent plates			
Crystal System	Monoclinic			
Space Group	$P2_1/c$			
Z	2			
a (Å)	8.249(1)	13.3166(3)	13.794(7)	14.0666(3)
b (Å)	6.0281(7)	4.54025(8)	4.462(3)	4.38905(8)
c (Å)	12.284(1)	11.8534(3)	11.963(7)	11.9563(3)
β (deg)	94.35(1)	110.8810(7)	110.23(4)	95.3328(7)
V (Å^3)	609.07(11)	669.6(3)	690.8(8)	734.97(3)
$R1$ [$F^2 > 2.0\sigma$ (F^2)]	0.054	0.0299	0.0447	0.0449
$wR2$ [All reflections]	0.140	0.0795	0.1328	0.1338

Device Fabrication and Thin Film Properties

The transistors were prepared by using a commercially available heavily doped n-type Si wafer with 300 nm SiO_2 insulator ($\varepsilon = 3.9$ and the capacitance of 11.5 nF cm^{-2}) as a gate.[S5] A passivation layer of tetratetracontane ($C_{44}H_{90}$, TTC) was evaporated ($\varepsilon = 2.5$ and 20 nm thickness with the capacitance of 106 nF cm^{-2}),[S6] and the resulting overall capacitance of the gate dielectric was 10.4 nF cm^{-2}. Then the indigo derivatives (45 nm) were deposited at a rate of 0.1 Å s^{-1} under a pressure of 10^{-3} Pa. Gold source and drain electrodes were evaporated through a shadow mask ($L/W = 100/1000$ µm) at a pressure of 10^{-3} Pa to accomplish the bottom-gate top-contact transistors (Figure 2). Transistor characteristics were measured with a Keithley 4200 semiconductor parameter analyzer under vacuum, and the mobility was evaluated from the transconductance in the saturated region. Figure S3 shows the gate leakage currents together with the drain current. Although the leakage current is not negligible in the subthreshold region, it does not influence the estimation of the mobilities particularly in **4**.
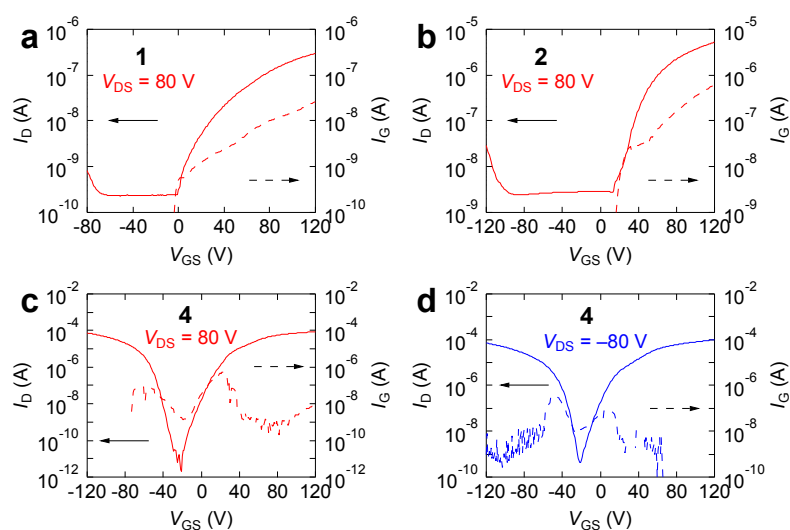

Fig. S3. Drain current (I_D, solid line) and gate leakage current (I_G, dotted line) in the $V_{DS} > 0$ region in the thin-film transistors of (a) **1**, (b) **2**, and (c) **4**, and those in the $V_{DS} < 0$ region in the thin-film transistors of (d) **4**.

All AFM images of thin films (a 45 nm of indigo compounds on a 20 nm of TTC) were taken by an SII scanning probe microscope system SPI3800N and SPA-300 by using a Si_3N_4 cantilever. X-ray diffraction analyses of all thin films (45 nm) on TTC (20 nm)|SiO_2 substrates were performed by X'pert-Pro-MRD using the θ - 2θ

technique with Cu-$K\alpha$ radiation for $2° \leq 2\theta \leq 50°$. Bragg's law ($n\lambda = 2d\sin\theta$, n : integer = 1) was used to estimate the d-spacing between layers of the thin films.

References

[S1] M. J. Frisch, G. W. Trucks, H. B. Schlegel, G. E. Scuseria, M. A. Robb, J. R. Cheeseman, G. Scalmani, V. Barone, B. Mennucci, G. A. Petersson, H. Nakatsuji,M. Caricato, X. Li,H.P. Hratchian, A. F. Izmaylov, J. Bloino, G. Zheng, J. L. Sonnenberg, M. Hada, M. Ehara, K. Toyota, R. Fukuda, J. Hasegawa, M. Ishida, T. Nakajima, Y. Honda, O. Kitao, H. Nakai, T. Vreven, J. A. Montgomery, Jr., J. E. Peralta, F. Ogliaro, M. Bearpark, J. J. Heyd, E. Brothers, K. N. Kudin, V. N. Staroverov, R. Kobayashi,J.Normand, K. Raghavachari, A. Rendell, J. C. Burant, S. S. Iyengar, J. Tomasi, M. Cossi, N. Rega, J. M. Millam, M. Klene, J. E. Knox, J. B. Cross, V. Bakken, C. Adamo, J. Jaramillo, R. Gomperts, R. E. Stratmann, O. Yazyev, A. J. Austin, R. Cammi,C. Pomelli, J. W. Ochterski, R. L. Martin, K. Morokuma, V. G. Zakrzewski, G. A. Voth, P. Salvador, J. J. Dannenberg, S. Dapprich, A. D. Daniels, O. Farkas, J. B. Foresman, J. V. Ortiz, J. Cioslowski, D. J. Fox, *Gaussian 09 (Revision B. 01)*, Gaussian, Inc., Wallingford CT, 2009.

[S2] T. Mori, A. Kobayashi, Y. Sasaki, H. Kobayashi, G. Saito, and H. Inokuchi, *Bull. Chem. Soc. Jpn.*, 1984, **57**, 627.

[S3] M. C. Burla, R. Caliandro, M. Camalli, B. Carrozzini, G. L. Cascarano, L. D. Caro, C. Giacovazzo, G. Polidori, D. Siliqi, and R. Spagna, *J. Appl. Crystallogr.*, 2007, **40**, 609.

[S4] G. M. Sheldrick, *Acta Crystallogr. Sect. A*, 2008, **64**, 112.

[S5] K. J. Baeg, Y. Y. Noh, J. Ghim, B. Lim, and D.Y.Kim, *Adv. Funct. Mater.*, 2008, **18**, 3678.

[S6] J. C. Ribierre, S. Ghosh, K. Takaishi, T. Muto, and T. Aoyama, *J. Phys. D*, 2011, **44**, 205102.